IEEE Access
Multidisciplinary | Rapid Review | Open Access Journal

Received August 16, 2019, accepted September 9, 2019, date of publication September 13, 2019,
date of current version September 26, 2019.

Digital Object Identifier 10.1109/ACCESS.2019.2940966

Effect of Electrical Load on Contact Welding Failure of Silver Tin Oxide Material Used in DC Electromechanical Relays

XU ZHANG, WANBIN REN, (Member, IEEE), ZHE ZHENG, AND SHUJUAN WANG
School of Electrical Engineering and Automation, Harbin Institute of Technology, Harbin 150001, China

Corresponding author: Wanbin Ren (renwanbin@hit.edu.cn)

This work was supported by the National Natural Science Foundation of China under Contract 51777039 and Contract 51377029.

ABSTRACT In order to clarify the contact welding failure mechanism of DC electromagnetic relay, a series of electrical endurance tests are carried out with the use of silver tin oxide material under resistive and capacitive load conditions. The typical waveforms of contact voltage and contact current during making and breaking resistive load and capacitive load (load capacitance of 1mF, 1.5mF, 2mF and 2.5mF) are obtained by the designed model switch. Further, the variations of sensitive electrical parameters such as bounce energy, contact resistance, static contact force and break arc energy during electrical endurance test are analyzed explicitly. It is found that the variations in sensitive electrical parameters is closely related to the electrical load type. In particular, under the capacitive load conditions, the sharp increase of each sensitive electrical parameter in the end of lifetime prognosticates the dynamic welding failure of silver tin oxide contact material. Finally, with the help of SEM (Scanning Electron Microscope) pictures of failed contacts, the surface erosion features of contact materials are mainly determined by the competition between the cathode arc and the anode arc. And the material transfer and distribution are the root reason for the contact welding failure of DC electromechanical relays.

INDEX TERMS Arc erosion, capacitive load, contact welding, resistive load, silver tin oxide material.

I. INTRODUCTION

Nowadays, silver based materials, including silver cadmium oxide Ag/CdO, silver tin oxide composite Ag/SnO_2, silver nickel AgNi, silver graphite AgC and so on are widespread used in all kinds of low voltage apparatus for switching current [1]–[3]. Silver-metal oxide composite materials offer many advantages over pure metals and alloys counterparts: higher resistance against welding, lower arc erosion and a significant lower tendency towards material transfer in DC switching circuits. Over the past years, many silver cadmium oxide contact materials have been replaced by silver tin oxide materials because of the toxicity of Cadmium. For this reason, silver tin oxide composite materials are extensively used in electrical switching devices like relays, installation and distribution switches, appliances, industrial controls, motor controls, and protective devices. According to incomplete statistics, in 2015 the silver consumption of China for manufacturing contact materials is about 1500 tons [4]. With the ever increased demand of high-reliability and long-life for electromechanical switches, the electrical performance of silver metal oxide material are urgent to be improved. It has been confirmed that contact welding, high contact resistance and severe contact erosion due to switching arc are the three major failure mechanisms for field engineering [5]–[9]. So, long-term stable performance of electrical contact materials is a fundamental precondition for reliability and lifetime of electronic and electrical application.

It is top-urgent to understand and determine the failure mechanisms of silver tin oxide composite material used in switching devices. Ever published research results have determined that the electric load (interrupting current and voltage), electric load type (resistive, inductive, capacitive, LED), contact force, contact size, environment (temperature, humidity, gas) have significant effect on electrical performance of contact materials. Particularly, capacitive load is a common switching duty in DC voltage networks [10]. The inrush current, occurred at the moment of contact touching, could increase the welding probability of contacts during making process [11], [12]. Therefore, the degradation process and

The associate editor coordinating the review of this manuscript and approving it for publication was Zhenliang Zhang.

typical features of silver tin oxide composite material in terms of the electrical endurance tests are always hot topics in this research field.

Morlin et al. [13] concluded that the reasonable cause of the contact welding is material transferred from anode to cathode caused by the short arc. Chen [9] also stated that strong contact welding is always associated with very short bounces (normally $<100\mu$s) on make or break but not all short make bounces cause strong welds. Compared with the lamp load testing results, it takes more operations to create strong welds in inductive load testing since the long break arc (especially gaseous phase arc) in inductive load can generate insulating films on the contact surface to prevent strong welds. Liu et al. [14] experimentally investigated the contact welding under the lamp load and pointed out the welding performance is influenced significantly by the anode material. In addition, the erosion and deposition of silver tin oxide composite material has been shown to be related closely to current [15], tin oxide particle size [16], metal oxide content [9] and [17], manufacturing process [17]–[19]. However, the root reason for contact dynamic welding in electrical endurance tests is not known completely.

The model switch concept is presented and adopted as the main experimental research and verification method [20]–[24]. The influence of mechanical parameters of switching devices and manufacturing process and methods of contact material in erosion resistance performance could be investigated easily with such kind of model switch. Particularly, Reichart *et.al* [25] introduced a new method to scan the topography of the anode and the cathode in correct spatial alignment with the use of confocal white light microscope. In order to guarantee the mechanical operation process provided by model switch roughly similar with the practical switching device, a test rig which allows for simulating contact mechanical operation and collecting electrical performance parameters during switching is present in this paper. The multidimensional data (including bounce energy, contact resistance, static contact force, break arc energy), which could characterize the degradation process of relay and contact material, are collected in real-time and analyzed explicitly during the electrical endurance test. The different degradation process under resistive and capacitive load conditions are presented innovatively and compared based on the variations of such sensitive parameters.

This paper is organized as follows. First, in Section II, the main function and specification of designed test rig for materials evaluation is described. The typical waveforms of contact voltage and contact current during making and breaking different capacitive load is plotted and explained in Section III. Besides, the variations in bounce energy, contact resistance, static contact force and break arc energy as a function of operation cycles are analyzed explicitly. Then, in Section IV, the eroded surface morphology and corresponding physical mechanism of contact welding are presented and speculated. Finally, the conclusion of the research is presented in Section V.

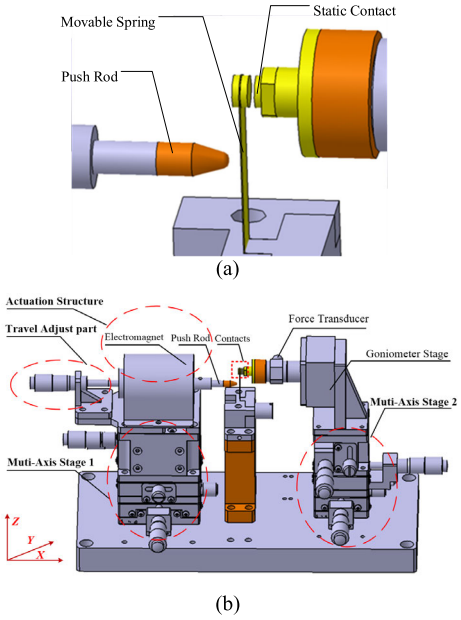

FIGURE 1. Mechanical structure of test rig. (a) Layout for a normally open contact. (b) Rhino-3D of test rig.

II. EXPERIMENTAL DETAILS

A. TEST RIG

The typical actuation of electromechanical relay is provided by the electromagnetic force. In order to simulate the mechanical operation of electromechanical relay quite closely, the mechanical structure of the test rig is designed as shown in Fig. 1. The whole experimental apparatus consists of three main modules, including the four-degrees-of-freedom motion structure, the measurement unit and the software control part. The horizontal actuation of the moving electrode is realized by a micro electromagnet connected with an insulated pushing rod. The actuation travel could be set by a micrometers head. The movable contact is attached to the free end of the leaf spring (beryllium bronze strip). The relative distance between pushing rod and the normally open contact pair in 'X' direction is determined by the Muti-Axis stage 1. The stationary contact is connected with the force sensor by the stationary strip, whose position in 'X' direction can be controlled by using Muti-Axis stage 2, thus the contact gap and the final contact force are both adjustable. All the above mechanical parameters have a resolution of 10μm. The mechanical structures are secured on the vibration isolation platform.

The contact voltage is measured by the method of resistor division, which provides a test resolution of 30mV. The contact current is measured by hall current sensor, which has the measurement range of 100A and the resolution of 50mA. The measurement of contact force is realized by a piezoelectric force sensor with the measurement range of 45N and the resolution of 1mN.

All above testing data including contact voltage, contact current and dynamic force are acquired by the commercial DAQ system (PCI1706, Advantech, Taiwan), which has a

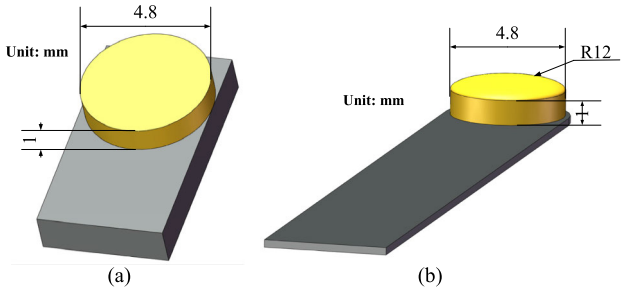

FIGURE 2. Rhino-3D of samples. (a) Static contact component. (b) Moveable contact component.

measurement resolution of 16 bits and a sampling frequency of 250kHz. The instrument is interfaced to a personal computer using serial port RS232. Data acquisition and logging process are controlled by a PC with the help of LabVIEW software specifically programmed for this purpose.

B. EXPERIMENTAL CONDITIONS

A series of electrical endurance tests are conducted to investigate the effect of capacitive load on contact welding of silver tin oxide type contact material. The rivet material is Ag/SnO_2 (88/12), and the applied additive is In_2O_3. The manufacturing process is power metallurgy method, which mainly includes powder blending, compaction, sintering, extrusion, wire drawing, and riveting. The Rhino-3D of experimental samples are shown in Fig. 2. As shown, the contact with flat surface is riveted with the short copper blade and the contact with cambered surface is riveted with the long beryllium bronze stripe. The samples are degreased using alcohol and distilled water in an ultrasonic cleaner, dried and carefully mounted in the test rig. When the welded contacts fail to re-open, that is to say, if the welding force is larger than the maximum opening force of 0.3N, then the experiments will be terminated. The circuit configuration is shown in Fig. 3.

In the figure, coil current is the current flowing through the coil of electromagnet, contact current is the current flowing through contact pair, contact voltage is the potential difference of contact pair, contact voltage-drop is the potential difference of contact pair after stable closure, and force signal is the output signal of dynamic force sensor. All experimental circuits in this paper, the supply voltage E is constant 28V, the resistance R_1 is 1.5Ω, R_2 is 0.1Ω, the contact current $I_{contact}$ is constant 18A after the contact pair is closed stably, and the duration of inrush current is determined by the load capacitance C. The stray inductance in the circuit is measured as 0.18mH. The details of the experimental conditions are listed in Table1.

TABLE 1. Experimental conditions.

Environment	Ambient temperature
Operating Frequency	1.5s on/1.5s off
Contact Voltage/Steady Current	DC28V/18A
Static Contact/Moveable Contact	Anode/Cathode
Initial Contact Force	1.8N
Initial Spring Force	0.3N
Initial Contact Gap	1mm
Maximum Opening Velocity	350mm/s
Number of Operations	Till welding of contacts
Capacitance (C)	1mF, 1.5mF, 2mF, 2.5mF
Resistance (R_1)/Resistance (R_2)	1.5Ω/0.1Ω
Stray Inductance	0.18mH

III. RESULTS AND DISCUSSION

A. TYPICAL CONTACT SWITCHING WAVEFORMS

Fig. 4 shows the representative examples of the measured variation of the contact voltage and contact current during contact making process respectively. In Fig. 4(a), the capacitance in the circuit is 2.5mF. The contact current could be expressed as

$$I_{contact} = \frac{E}{R_1 + R_2 + R_c}\left[1 + \frac{R_1}{R_2 + R_c}\exp(-\frac{t}{\tau})\right] \quad (1)$$

in formula (1), τ is:

$$\tau = \frac{R_1(R_2 + R_c)C}{R_1 + R_2 + R_c} \quad (2)$$

where E is the supply voltage, here is 28V. R_1 is 1.5Ω, R_2 is 0.1Ω, load capacitor C is 2.5 mF, and R_c is contact resistance.

At the initial contact process, the contact current increases exponentially to 95A, afterwards the value continuously declines to 25A. This is attributed to the occurrence of a long contact bounce of 400μs. When the contact re-closes, the second inrush current of 55A and subsequent steady value of 18A are observed. The corresponding whole contact voltage shifts from 28V to 0.2V accompanied with an oscillation. We define the product of contact voltage and contact current in terms of contact bounce is the bounce energy, then it is written by

$$Q = \int_{t_0}^{t_1} uidt = \sum_{i=1}^{n} U_i I_i \Delta t = \frac{1000}{f}\sum_{i=1}^{n} U_i I_i \quad (3)$$

where f is sampling frequency, U is contact voltage, and I is contact current. t_0 represents the moment of the first contact. t_1 represents the moment of the moment of bounce end. So it is calculated as 252.4mJ. In Fig. 4(b), the load is resistive (capacitance is 0mF). At the initial contact process, the contact current increases to 10A and then holds for about 400μs, the same time as contact bounce. Then the current eventually stabilizes at 18A, and there is no inrush phenomenon during the making process. The bounce energy is 50.24mJ.

Three distinct examples of measured contact voltage and current waveforms in contact breaking process are shown in Fig. 5. In Fig. 5(a), at the beginning of 40μs, an abrupt transition to a significantly low level almost zero current occurs, meanwhile, a hump of contact voltage (10V) is observed. This is a situation where a certain amount of inductance parallel to the contact pair. Because the hump voltage is lower than the minimum electric arc voltage (for Ag/SnO_2 material is about 12V), then the arc might not be ignited. After that, the contact voltage increases from 5V to the DC supply

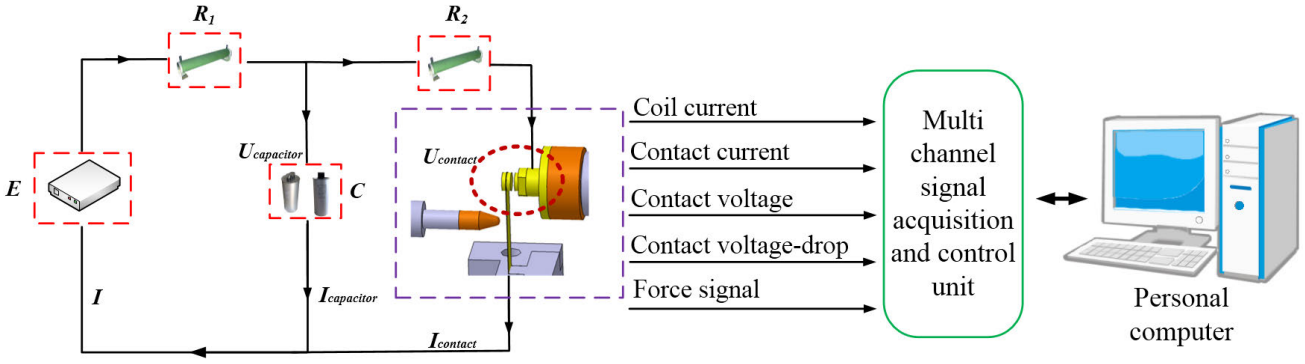

FIGURE 3. Schematic of the experimental circuit.

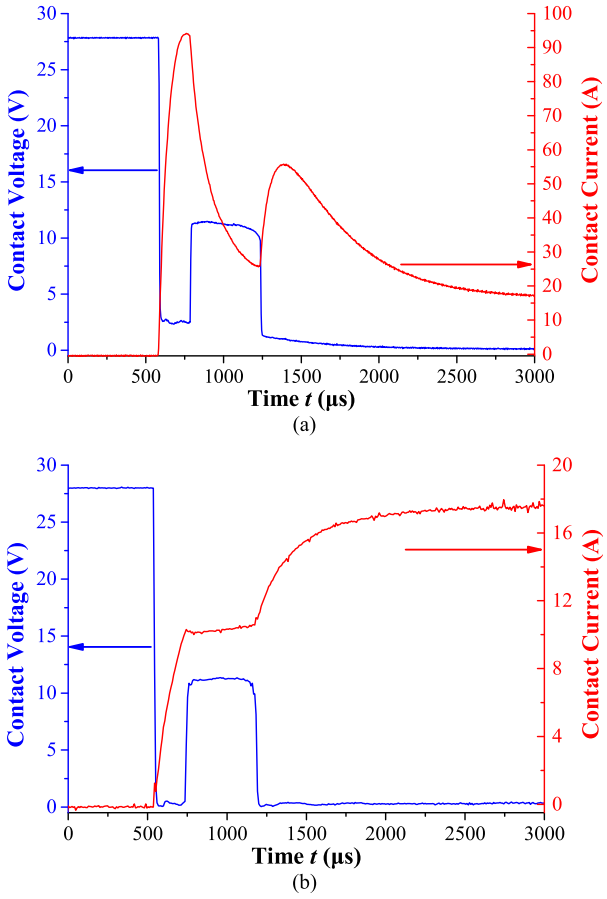

FIGURE 4. The representative examples of contact voltage and contact current during making process. (a) C = 2.5mF (b) C = 0mF.

potential exponentially. However, as shown in Fig. 5(b), when the contact voltage reaches 15V, the contact current shifts from zero to 7A instantaneously, the gap is re-striked and the arcing duration is 15ms. Afterwards, the circuit is open and the contact voltage increases to the DC supply potential exponentially again. We call the integral product of contact voltage and current during restrike as the break arc energy. The break arc energy in Fig. 5(b) is 1591.2mJ. Fig. 5(c) is a typical waveform of breaking process with resistive load. The break arc energy of Fig.5(c) is 455.54mJ. It's worth mentioning that during the electrical endurance test, for the capacitive load case, the arcing phenomenon occurs less. However, for the resistive load case, the arcing phenomenon always exists.

B. EFFECT OF CAPACITANCE ON CONTACT MAKING AND BREAKING PROCESS

Fig. 6 shows the transient waveforms of contact current and contact voltage for contact making load capacitance of 1mF, 1.5mF, 2mF and 2.5mF. In the initial 100μs period, the contact current sharply increases with the same trend. The decline of current is direct proportional to the load capacitance value corresponding to the bounce duration of 400μs to 800μs. It is noticed that the current keeps zero value for nearly 200μs when the capacitance is 1mF. Next, the current continues to increase when the contact is re-closed. Particularly, the initial restoring current is higher than the steady current of 18A when the capacitance is 2.5mF. It is attributed that the released quantity of electric charge has no substantial difference before the contact bounce, while the remained electric charge increased with the higher capacitance after the bounce. The value of bounce energy is calculated as 95.07mJ, 168.97mJ, 219.99mJ and 252.4mJ for the capacitance of 1mF, 1.5mF, 2mF and 2.5mF respectively. Therefore, the bounce energy could be extended effectively with respect to the increased capacitance.

Fig. 7 shows the transient waveforms of contact voltage for contact breaking load capacitance of 1mF, 1.5mF, 2mF and 2.5mF. The similar humps of contact voltage, which are no more than 10V in the beginning, is observed for different load capacitance. After that, the voltage all increases exponentially to the open voltage of 28V. The recovering duration of voltage is shorten with respect to the lower capacitance. As stated, the contact voltage is equal to the capacitance voltage. The charging time constant could be written as the product of resistance and capacitance. So, the stabilization time is remarkably affected by the load condition.

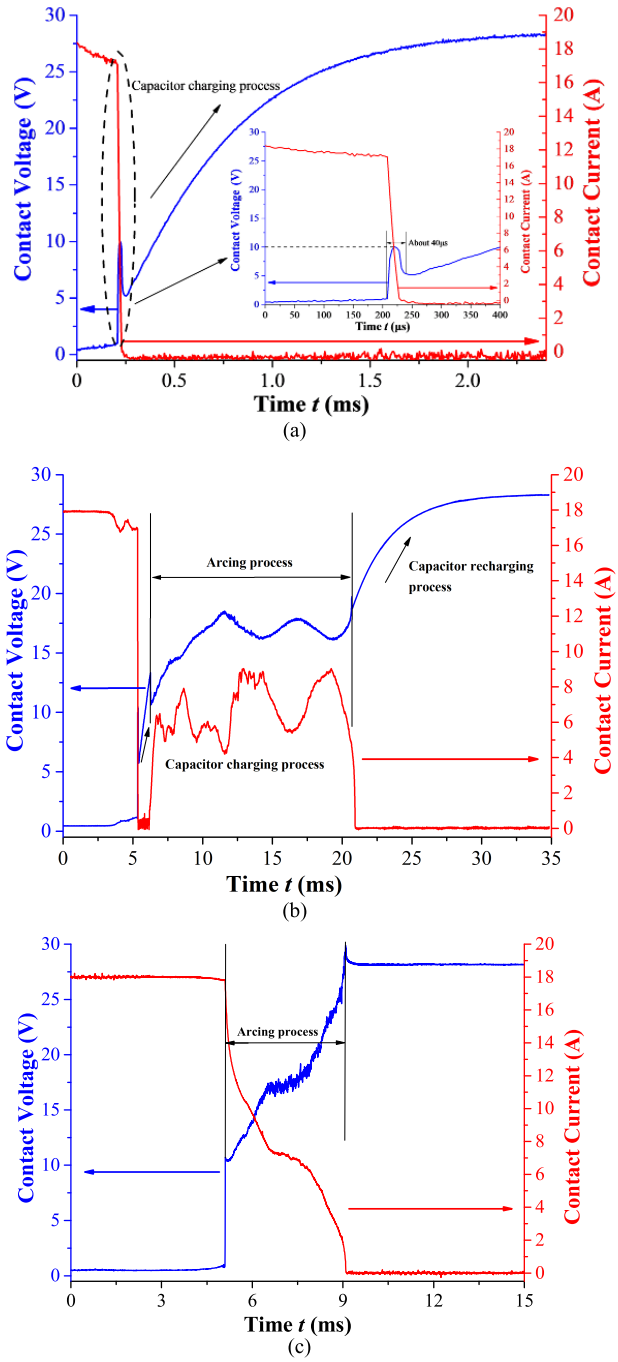

FIGURE 5. Three distinct examples of contact voltage and contact current waveforms of contact breaking. (a) Without arcing phenomena, C = 2.5mF (b) Arcing phenomena, C = 2.5mF (c) Arcing phenomena, C = 0mF.

C. ELECTRICAL ENDURANCE TEST RESULTS

The electrical lifetime of contacts is also called the operation cycles corresponding to the contacts occurred welding failure. Three electrical endurance tests were done for load capacitance of 0mF, 1mF, 1.5mF, 2mF and 2.5mF, respectively. The error bars of electrical lifetime are shown in Fig. 8.

As shown in Fig. 8, the electrical lifetime of contact is the longest for the resistive load case (capacitance is 0mF), followed by the capacitance of 1mF, 1.5mF and 2mF. For the capacitance of 2.5mF case, the lifetime is the shortest of all, only about 1/10 of the resistive condition.

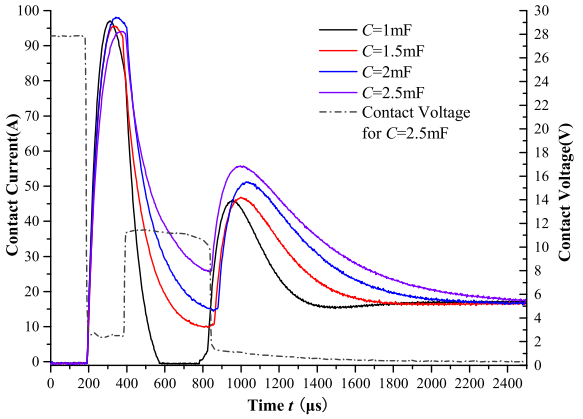

FIGURE 6. The transient waveforms of contact current for contact making of a series of capacitive loads (E = 28V, I = 18A, I_{rush} = 95A).

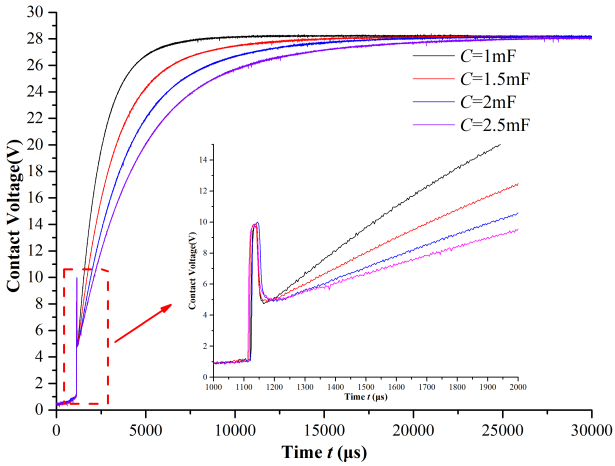

FIGURE 7. The transient waveforms of contact voltage for contact breaking of a series of capacitive loads (E = 28V, I = 18A, I_{rush} = 95A).

During each electrical endurance test, the bounce energy, the contact resistance, the static contact force and the break arc energy are recorded explicitly by using above mentioned test rig. The test results with middle lifetime in three electrical endurance tests are analyzed for each load capacitance. In order to gain the obvious change trend of each parameter, the average of 200 consecutive values are calculated and plotted with red line in Fig. 8-11.

1) BOUNCE ENERGY

The detailed variations in bounce energy of contact as a function of operation cycles is shown in Fig. 9(a). The distribution probability of bounce energy are shown in Fig. 9(b) with the use of data in Fig. 9(a). The mean value of bounce energy is calculated as 49.79mJ, 137.94mJ, 208.62mJ, 243.65mJ and 293.82mJ for the capacitance of 0, 1mF, 1.5mF, 2mF and 2.5mF respectively. Under the resistance condition, more than 90% of the bounce energy is distributed in the range of 39mJ and 63mJ, which means the least fluctuation in above all load

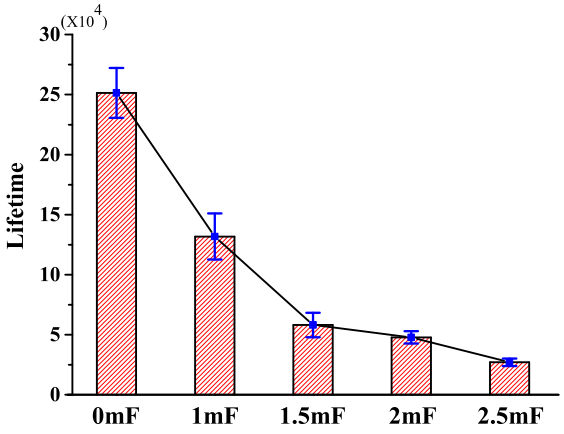

FIGURE 8. The electrical lifetime of contacts for a series of capacitive loads. The red column the average.

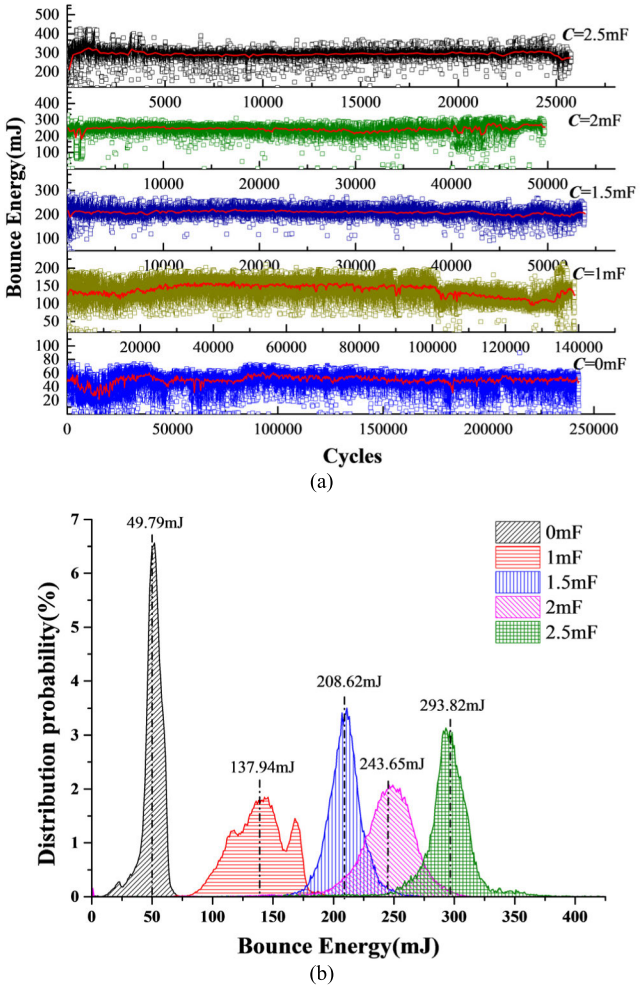

FIGURE 9. Variations in bounce energy of silver tin oxide contact material as a function of operation cycles for a series of capacitive loads. The red line is the average of 200 numbers. (a) Bounce energy. (b) Distribution probability.

conditions. In contrast, when the capacitance is increased to 2mF, the bounce energy fluctuates sharply and more than 90% values are distributed between 209mJ and 281mJ. It indicates

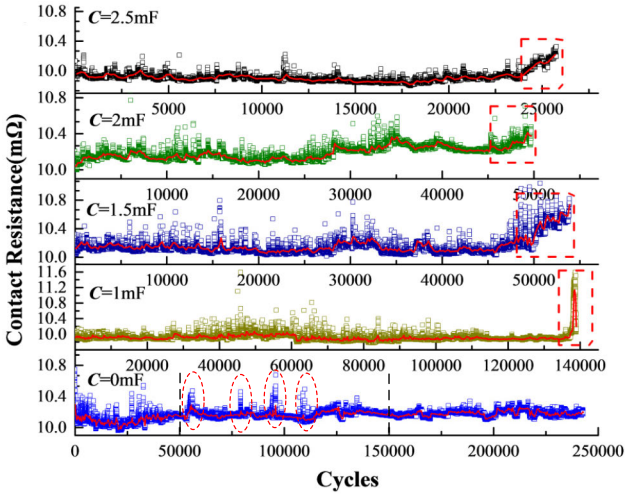

FIGURE 10. Variations in contact resistance of silver tin oxide contact material as a function of operation cycles for a series of capacitive loads. The red line is the average of 200 numbers.

that the bounce energy keeps relatively stable and accompanied by small fluctuations during the individual electrical endurance test, and the main reason for its small fluctuations is that the mechanical motion of the contact making process cannot be absolutely consistent, so the bounce time is changeable to some extent.

In addition, it is noticed that the mean value of bounce energy also increases with the increase of load capacitance value. It means that the higher load capacitance could result into more serious surface erosion and welding of the material surface, and subsequently shorten the lifetime in the electrical endurance test.

2) CONTACT RESISTANCE

Fig. 10 shows the variations in contact resistance of silver tin oxide contact material as a function of operation cycles for capacitance value of 0, 1mF, 1.5mF, 2mF and 2.5mF. The initial contact resistance keeps at around 10mΩ. For the resistive load condition, the contact resistance always remain at about 10.1mΩ during the whole test. However, for all the capacitive loads, the contact resistance is stable within 90% of the electrical endurance test, and then increases sharply within the end of the test (shown in the red box in the figure). Particularly, the contact resistance increases from 10mΩ to 11.6mΩ when C = 1mF.

The above results indicate that the behavior of contact resistance in the electrical endurance test is closely related to the electrical load type. It could be considered that the rapid increase of contact resistance under the capacitive load condition is the main degradation feature of contact material. While, there is no such clear prediction for the resistive load condition.

3) STATIC CONTACT FORCE

The variations in static contact force as a function of operation cycles for a series of capacitive loads are shown in Fig. 11.

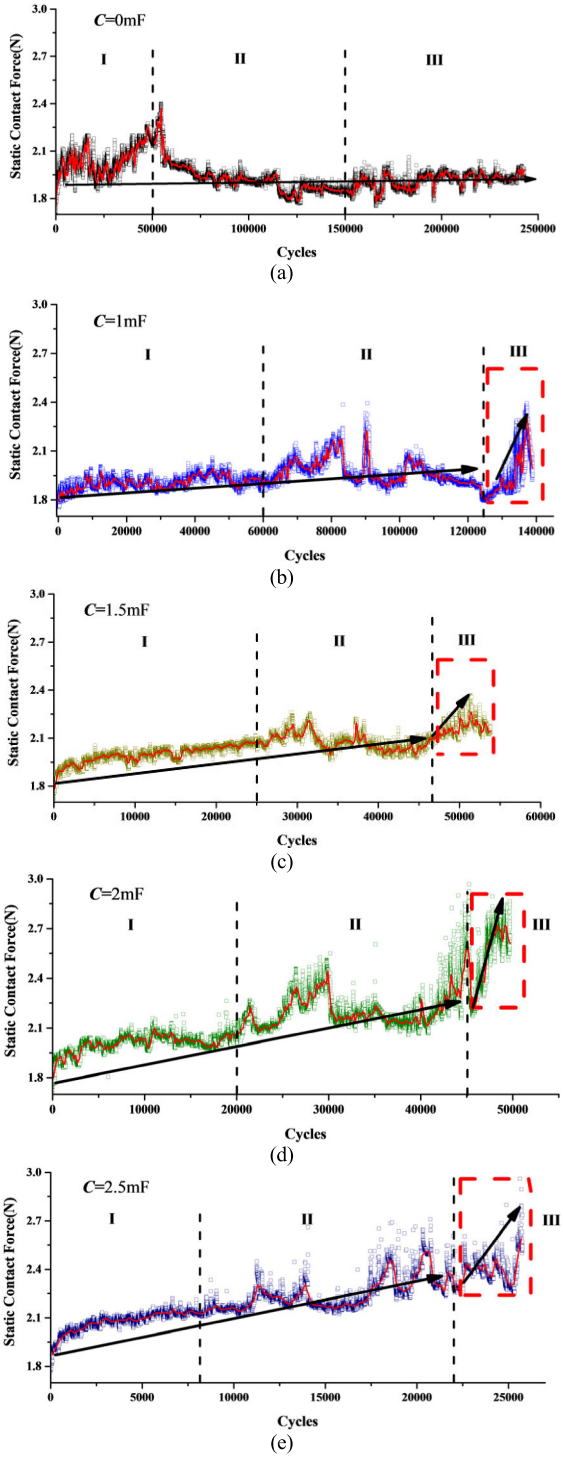

FIGURE 11. Variations in static contact force of silver tin oxide contact material as a function of operation cycles for a series of capacitive loads. The red line is the average of 200 numbers. (a) C = 0mF (b) C = 1mF (c) C = 1.5mF (d) C = 2mF (e) C = 2.5mF.

For all the capacitive load condition, the observed trends of static contact force appears similar with the behavior of contact resistance. In the early of electrical endurance test, the static contact force increases slowly, while in the remained

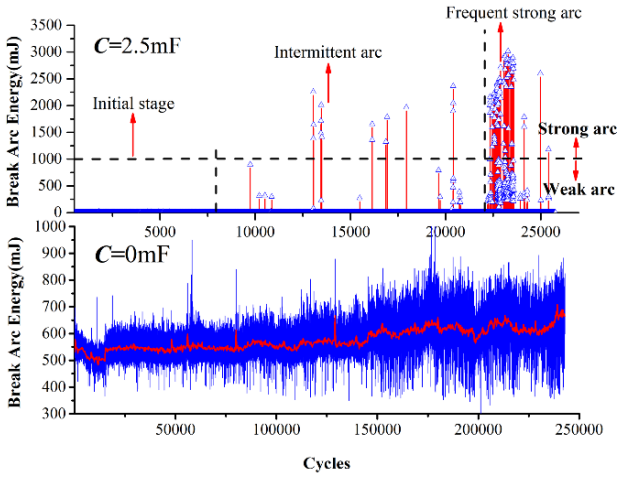

FIGURE 12. Variations in break arc energy of silver tin oxide contact material as a function of operation cycles for the resistive load and the capacitive load. The red line is the average of 200 numbers.

lifetime there is a rapid increment. It is noted that the average value of static contact force in the 10% end of lifetime test is 1.95N, 2.17N, 2.53N and 2.40N, which corresponds to the load capacitance of 1mF, 1.5mF, 2mF and 2.5mF respectively. The static contact force eventually increases about 8%, 21%, 41% and 33%, respectively, compared with the initial value of 1.8N. However, for the resistive load, the static contact force increases rapidly from 1.8N to 2.4N during the initial 50,000 cycles, and then drops to about 1.9N and remains relatively stable until the electrical endurance test terminates. It indicates that the change of static contact force could also reflect the degradation process of contact material in the capacitive load condition. The substantial increase of static contact force relates to the higher load capacitance closely.

4) BREAK ARC ENERGY

Fig. 12 shows the variations in break arc energy of contact material as a function of operation cycles for the resistive load case (capacitance is 0mF) and the capacitive load case (capacitance is 2.5mF). For the resistive load, the arc phenomenon always exists in the contact breaking process. The break arc energy fluctuates between 500mJ and 600mJ during the initial time, while in the end of the electrical endurance test, the highest break arc energy increases into 900mJ. For the capacitance of 2.5mF case, there is no breaking arc within the initial 8000 cycles. We further define 1000mJ as the threshold value of strong arc. The intermittent arc phenomena is observed with the maximum break arc energy of 2366mJ between 8000 cycles and 22,000 cycles.

Afterwards, the frequent strong arc with the maximum break arc energy of 3016mJ is noticed from 22,000 cycles until the electrical endurance test terminates.

It can be found that the arc phenomenon exists in the whole endurance test for the resistive load case. While for the capacitive load, the intermittent arc phenomenon is observed during contact breaking. The arc occurrence frequency and

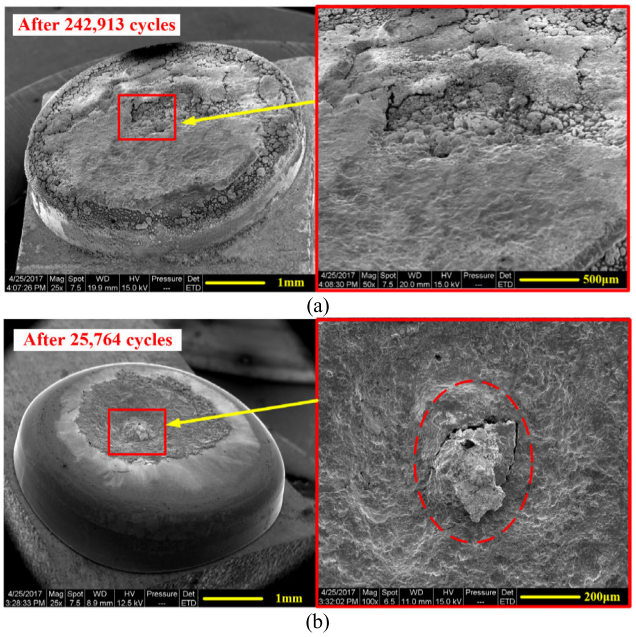

FIGURE 13. SEM pictures of anode surfaces after electrical endurance test (a) welded after 242,913 cycles, C = 0mF (b) welded after 25,764 cycles, C = 2.5mF.

the break arc energy increase significantly with the endurance test proceeding.

IV. FAILURE MECHANISM ANALYSIS

In order to get better insight about the observed changes in sensitive electrical parameters of contacts before welding failure, the surface morphologies of failure contact pairs are captured by using SEM (Scanning Electron Microscope).

Fig. 13 shows the SEM pictures of anode surfaces after electrical endurance test. For the resistive load (C = 0mF), the whole surface of anode contact is eroded seriously, the cracks distributes over the whole surface, and there are a lot of metal splashes on the contact edge, as shown in Fig. 13(a). For the capacitance of 2.5mF case, the arc erosion mainly occurs at the center of the contact surface, and the eroded zone seems like a huge pit with a pip in the center, which accounts for about half of the whole contact surface, as shown in Fig. 13(b). There is an obvious fracture cross section and delamination layer in the pit center, which corresponds to the final welding zone.

The SEM pictures of cathode surfaces after electrical endurance test are shown in Fig. 14. For the resistive load (C = 0mF), the surface morphology of cathode is similar to the anode. As shown in Fig. 14(a), there are a large number of pores and coral-like structures at the edge of contact. The surface morphology of silver tin oxide contact material under switching capacitive load is shown in Fig. 14(b). The erosion area on the cathode surface looks like a large pip, which is different from the contact surface morphology shown in Fig. 13(b). At the top of pip, there is a ''crater'' type erosion pit and associated fracture

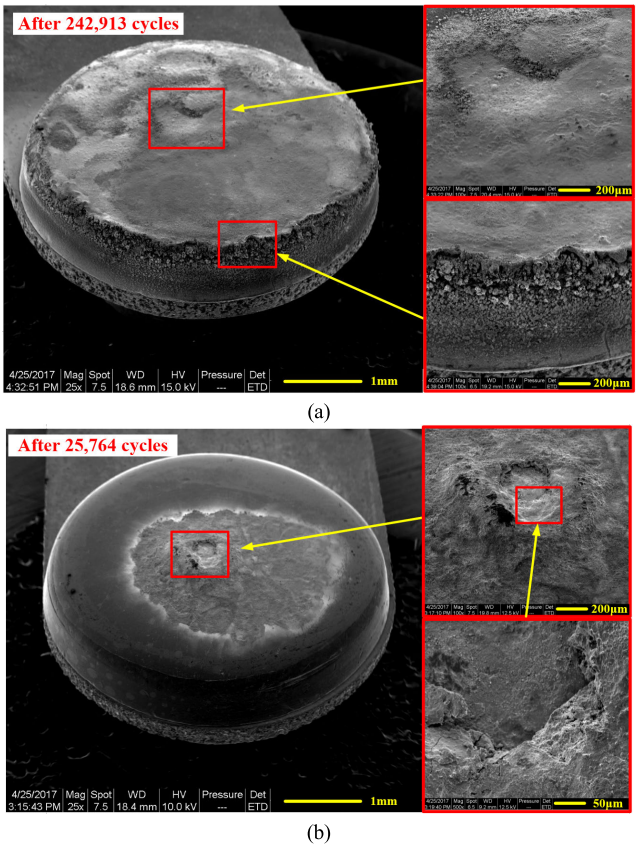

FIGURE 14. SEM pictures of cathode surfaces after electrical endurance test (a) welded after 242,913 cycles, C = 0mF (b) welded after 25,764 cycles, C = 2.5mF.

cross section. This exactly corresponds to the welding trace in Fig. 13(b).

It is noticed that the contact surface morphology caused by arc erosion are obviously different under the two electrical load types of resistance and capacitance. Material mass net transfer is directly induced by cathode arc in the breaking process and anode arc in the making process [26]–[29]. For the resistive load (C = 0mF), cathode arc in the breaking process and anode arc in the making process occur in each operation cycle, and then the material mass transfer is also bidirectional. Meanwhile, the random arcing and splash feature results in the erosion trace distributed within the whole surface and the failed contact surface keeps relatively flat. However, the anodic arc behavior dominates the whole electrical endurance test with absolute advantage for the capacitive load (C = 2.5mF). So, a large pit on the anode surface and a clear crater is observed on the cathode surface. In addition, for the resistive load case (capacitance is 0mF) the contact lifetime is 242,913 times, while for the capacitance of 2.5mF case, the life span is the shortest of all, only 25,764 times, which is about 1/10 of the resistive load condition. Therefore, the arcing erosion features depend not only on the current load type but also the number of operation cycles.

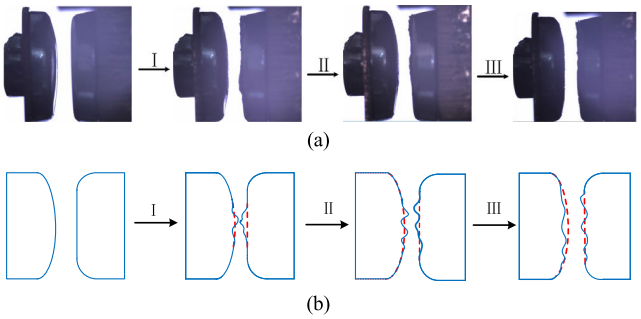

FIGURE 15. The degradation process of contact surface at the resistive load condition. (a) Pictures. (b) Schematic.

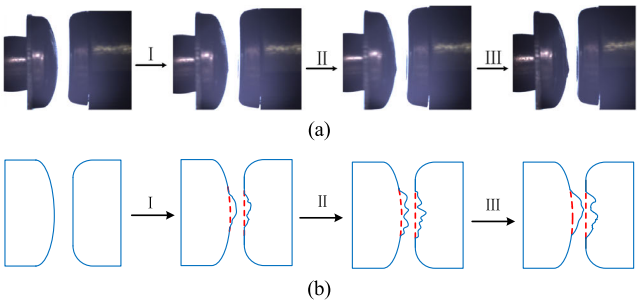

FIGURE 16. The degradation process of contact surface at the capacitive load. (a) Pictures. (b) Schematic.

Fig. 15 shows the degradation process of contact surface at resistive load. The whole process could be divided into three stages according to the operation cycles (shown in Fig. 11). The first stage is the contact material accumulation period. The sphere-plane contact feature causes the contact zone located in the geometry center of the contact. The arc repeatedly erodes the central region, and the materials are continuously heated, melted, cooled and solidified, the contact area varies with the material transfer in this region. The associated contact resistance fluctuates between 10mΩ and 10.7mΩ during the initial 5000 cycles, as shown in Fig. 10. With the material accumulates in the central area, the contact gap decreases gradually, and the static contact force increases slowly from 1.8N to 2.4N, as shown in Fig. 11.

The second stage is the contact material dispersing period. With the accumulation of materials in the central area, the arc mainly erodes this bulge area, and the material accumulated in the central area begins to disperse around, the contact gap increases gradually, and the static contact force decreases from 2.4N to 1.9N during 5000 cycles and 15000 cycles (shown in Fig. 11). The dispersion of materials in the central area leads to the increase of the contact area and material transfer at many points on the contact surface. When two formed high asperities contact each other, the rapid decrease of contact area results the contact resistance increase suddenly and ignites the breaking arc. The direct consequence is the melting of early formed high asperities. This splash behavior expends the contact area again and results the associated contact resistance decrease again, as shown in the red ellipse dotted line in Fig. 10(C = 0mF). After the forming and dispersing of such high asperities, the material accumulated in the central area gradually expands to the whole surface, and the contact resistance is gradually stabilized.

The third stage is the contact surface flattening period. From 15,000 cycles to the end of electrical endurance test, the material accumulated in the central area transfer to the whole surface. The arc could occur randomly at the high asperities of the whole surface, so that the arc erosion traces are distributed within the whole surface of contacts. This maybe the root reason for the original cambered cathode surface changing into flat shape after experiments (shown in Fig. 14(a)). In this period, the contact resistance remains stable at about 10.1mΩ and the static contact force almost keeps 1.9N, as shown in Fig. 10 and Fig. 11.

The degradation process of contact surface at capacitive load is shown in Fig. 16. Similar to the resistive load case, the whole process can be divided into three stages, the first stage is the contact material unidirectional transfer period. The contact surface is eroded gradually with the strong short arc resulted by the bounce and inrush current during the initial 8,000 cycles. As shown in Fig. 12, there is only anodic arc occurred in the making process during this period. The anodic arc caused by bounce makes the material transfer from anode to cathode. With the material consecutive accumulation on the cathode, the contact gap decreases gradually and the static contact force rises slowly, as shown in Fig. 11.

The second stage is the intermittent reverse transfer period. During 8,000 cycles and 22,000 cycles, the further decrease of contact gap results the dielectric recovery strength weaken.

Then, the occurrence of breaking arc causes material reverse transfer from the cathode to the anode. So, the contact gap increases again and the dependent static contact force also decreases remarkably. Once the breaking arc disappears, the anodic arc in making process causes the material transfers to the cathode again. Therefore, there is a cyclic fluctuation of static contact force in the second stage, which means ''increase-decrease-increase'', as shown in Fig. 11.

The third stage is the frequent welding period. The frequent strong arc is the main cause of the degradation of contact surface morphology from 22,000 cycles to the electrical endurance test terminates, as shown in Fig. 12. The material between contact pair is continuously heated, melted, and solidified. The high asperities begin to form in the huge pit on the contact surface. It brings out the further decrease of contact gap and the rapid rise of static contact force, as shown in Fig. 11. Meanwhile, the frequent strong arc increases the melting area of the contact until the contacts fail to re-open.

V. CONCLUSION

In this paper, the variations in bounce energy, contact resistance, static contact force and break arc energy of silver tin

oxide contact material are recorded with the use of designed model switch during the electrical endurance test. The possible welding failure mechanisms of material switching different electrical load conditions are introduced.

(1) Switching the capacitive load results in the increase of bounce energy during contact making process, which could make the contacts easier to welding failure than the resistive load condition. So, the higher load capacitance could lead to the decrease of the contact lifetime in the electrical endurance test.

(2) Compared with the results of contact material under the resistive load conditions, the variations in contact resistance, the static contact force and frequency of arc occurrence increased sharply in the end of lifetime for the capacitive load. The occurred micro bulges in the eroded contact surface is the root reason for the increase of static contact force and contact resistance.

(3) The arc erosion morphology of contact materials is different distinctly for mentioned electrical load types. For the resistive load, the failed contact surface is relatively flat and the eroded traces distributed throughout the surface. However, for the capacitive load, the erosion area only exists within the center of surface and the substantial mass transfer is observed. The difference of erosion morphology is mainly determined by the combined actions of cathode arc in the breaking process and anode arc in the making process. The occurred pits and pips on the contact surfaces are more likely to cause strong welding.

(4) The degradation process of silver tin oxide contact material for the resistive load condition could be divided into the accumulation period, the dispersing period and the surface flattening period. However, the degradation process of contact material for the capacitive load condition could be divided into the unidirectional transfer period, the intermittent reverse transfer period and the frequent welding period.

REFERENCES

[1] M. Shen, W. Cote, and L. Gould, "A historic review of Ag-MeO materials," in *Proc. 32nd Holm Conf. Electr. Contacts*, Boston, MA, USA, 1986, pp. 71–76.

[2] P. G. Slade, *Electrical Contacts: Principles and Applications*. New York, NY, USA: CRC, 2014, pp. 792–793.

[3] M. Braunovic, V. V. Konchits, and N. K. Myshkin, *Electrical Contacts: Fundamentals, Applications and Technology*. London, Britain: Taylor & Francis, 2006, pp. 112–115.

[4] D. Cui, "Development analysis for China electric contact material market," in Chinese, *Electr. Eng. Mater.*, vol. 2, no. 2, pp. 24–28, Jun. 2016.

[5] Z.-K. Chen and G. J. Witter, "Electrical contacts for automotive applications: A review," *IEICE Trans. Electron.*, vol. E87-C, no. 8, pp. 1248–1254, 2004.

[6] T. Mützel and R. Niederreuther, "Advanced silver-tinoxide contact materials for relay application," in *Proc. 26th Int. Conf. Elect. Contacts*, Beijing, China, May 2012, pp. 194–199.

[7] T. Mützel, M. Bender, and F. Heringhaus, "Thermo-mechanical stress in electrical contacts due to arcing events," in *Proc. 28th Int. Conf. Electr. Contacts*, Edinburgh, Scotland, 2016, pp. 373–378.

[8] G. Witter and Z. Chen, "Dynamic welding resistance of silver and silver metal oxides," in *Proc. 19th Int. Conf. Electr. Contacts*, Arlington, TX, USA, 1998, pp. 355–359.

[9] Z. Chen, "The effect of silver composition and additives on switching characteristics of AgSnO2 type contacts for the automotive inductive loads," in *Proc. 51st IEEE Holm Conf. Electr. Contacts*, Chicago, IL, USA, Sep. 2005, pp. 35–41.

[10] H. Liang, H. Yu, G. Ma, Z. Cai, Y. Tang, and C. Zhao, "Surge load experiment design and results analysis of relay," in *Proc. IEEE 61st Holm Conf. Elect. Contacts*, San Diego, CA, USA, Oct. 2015, pp. 107–110.

[11] X. Zhang, Z. Zheng, W. Ren, and Z. Zhou, "An experimental investigation of dynamic welding mechanism of contacts used in low current switching devices," in *Proc. 64th IEEE Holm Conf. Elect. Contacts*, Albuquerque, NM, USA, Oct. 2018, pp. 488–494.

[12] W. Ren, X. Zhang, T. Wang, and J. Wei, "Study on switching characteristics and associated degradation mechanism of contact material under capacitive load," *IEEE Trans. Compon., Packag. Manuf. Technol.*, vol. 8, no. 11, pp. 2030–2038, Nov. 2018.

[13] L. Morin, N. B. Jeman, and D. Jeannot, "Make arc erosion and welding in the automotive area," *IEEE Trans. Compon. Packag. Technol.*, vol. 23, no. 2, pp. 240–246, Jun. 2000.

[14] L. Xiangjun, F. Xiao, and F. Hongjun, "Welding characteristics of Ag-based contact material under automobile lamp load," in *Proc. 49th IEEE Holm Conf. Elect. Contacts*, Washington, DC, USA, Sep. 2003, pp. 145–149.

[15] J. Swingler and W. J. McBride, "The erosion and arc characteristics of Ag/CdO and Ag/SnO_2 contact materials under DC break conditions," *IEEE Trans. Compon., Packag., Manuf. Technol., Part A*, vol. 19, no. 3, pp. 404–415, Sep. 1996.

[16] M. Zhang, X.-H. Wang, X.-H. Yang, J.-T. Zou, and S.-H. Liang, "Arc erosion behaviors of AgSnO_2 contact materials prepared with different SnO_2 particle sizes," *Trans. Nonferrous Met. Soc. China*, vol. 26, no. 3, pp. 783–790, Mar. 2016.

[17] P. Braumann and A. Koffler, "The influence of manufacturing process, metal oxide content, and additives on the switching behaviour of Ag/SnO_2 in relays," in *Proc. 50th IEEE Holm Conf. Elect. Contacts 22nd Int. Conf. Elect. Contacts Elect. Contacts*, Seattle, WA, USA, Sep. 2004, pp. 90–97.

[18] V. Behrens, T. Honig, A. Kraus, R. Michal, K. Saeger, R. Schmidberger, and T. Staneff, "An advanced silver/tin oxide contact material," *IEEE Trans. Compon., Packag., Manuf. Technol., Part A*, vol. 17, no. 1, pp. 24–31, Mar. 1994.

[19] E. Streicher, C. Leung, and D. Fitzgerald, "Arc affected surface composition changes in silver tin oxide contacts," in *Proc. 54th IEEE Holm Conf. Elect. Contacts*, Orlando, FL, USA, Oct. 2008, pp. 301–307.

[20] A. R. Neuhaus, W. F. Rieder, and M. Hammerschmidt, "Influence of electrical and mechanical parameters on contact welding in low power switches," *IEEE Trans. Compon. Packag. Technol.*, vol. 27, no. 1, pp. 4–11, Mar. 2004.

[21] J. W. McBride, "Electrical contact bounce in medium-duty contacts," *IEEE Trans. Compon., Hybrids, Manuf. Technol.*, vol. 12, no. 1, pp. 82–90, Mar. 1989.

[22] A.R. Neuhaus, T. Felkel, A. Hammerschmid, and W. F. Rieder, "The influence of kinetic parameters on failure mechanisms caused by material transfer," in *Proc. 50th IEEE Holm Conf. Elect. Contacts 22nd Int. Conf. Elect. Contacts Elect. Contacts*, Seattle, WA, USA, Sep. 2004, pp. 528–534.

[23] X. Yang, J. Huang, Z. Li, J. Liu, Q. Wang, and M. Hasegawa, "The preceding voltage pulse and separation welding mechanism of electrical contacts," *IEEE Trans. Compon., Packag., Manuf. Technol.*, vol. 6, no. 6, pp. 846–853, Jun. 2016.

[24] D. Gonzalez, M. Hopfeld, F. Berger, and P. Schaaf, "Investigation on contact resistance behavior of switching contacts using a newly developed model switch," *IEEE Trans. Compon., Packag., Manuf. Technol.*, vol. 8, no. 6, pp. 939–949, Jun. 2018.

[25] M. Reichart, C. Schrank, and G. Vorlaufer, "Investigation of material transfer by 3D precision alignment of topographical data of electrical contact surfaces," in *Proc. 54th IEEE Holm Conf. Elect. Contacts*, Orlando, FL, USA, Oct. 2008, pp. 313–318.

[26] L. H. Germer, "Physical processes in contact erosion," *J. Appl. Phys.*, vol. 29, no. 7, pp. 1067–1082 Jul. 1958.

[27] P. G. Slade, "Opening electrical contacts: The transition from the molten metal bridge to the electric arc," *IEICE Trans. Electron.*, vol. E93-C, no. 9, pp. 1380–1386, 2010.

[28] Z.-K. Chen, H. Mizukoshi, and K. Sawa, "Contact erosion patterns of Pd material in DC breaking arcs," *IEEE Trans. Compon., Packag., Manuf. Technol., Part A*, vol. 17, no. 1, pp. 61–67, Mar. 1994.

[29] Z.-K. Chen and K. Sawa, "Effect of arc behaviour on material transfer: A review," *IEEE Trans. Compon., Packag., Manuf. Technol., Part A*, vol. 21, no. 2, pp. 310–322, Jun. 1998.

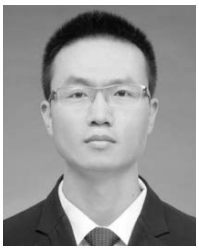

XU ZHANG was born in 1992. He received the B.S. degree from the Harbin Institute of Technology, China, in 2016, where he is currently pursuing the Ph.D. degree with the School of Electrical Engineering and Automation. His research interest includes the evaluation method of electrical performance for electrical contact materials.

WANBIN REN (M'12) was born in 1977. He received the M.S. and Ph.D. degrees from the Harbin Institute of Technology, Harbin, China, in 2003 and 2006, respectively, where he is currently a Professor with the School of Electrical Engineering and Automation. His current research interests include electrical contact theory and measurement techniques for electrical contact materials.

ZHE ZHENG, photograph and biography not available at the time of publication.

SHUJUAN WANG, photograph and biography not available at the time of publication.